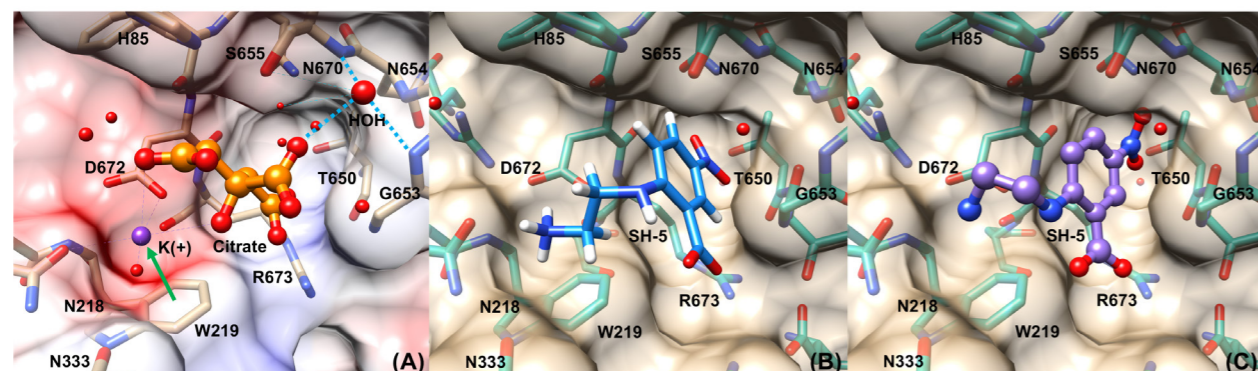


## Fragment-Based Discovery of the First Non-Peptidyl Inhibitor for Dipeptidyl Aminopeptidase with Chymotrypsin-Like Domain from Pathogens

Since the emergence of humans, the battle between humans and infectious diseases has continued. Salvarsan is well-known as the first synthesized antimicrobial, developed in 1911. Until then, humans had no effective countermeasures against pathogens, but thereafter, humans fought off infections by continuing to develop new antimicrobials. However, this has led to the emergence of antimicrobial resistance (AMR), which has become a global problem. AMR related infectious diseases and chronic periodontitis are caused by infection with non-fermenting gram-negative rods (NFGNRs). NFGNRs require peptides for their growth instead of carbohydrates. Consequently, peptide digestion or metabolism pathways are assumed to be potential antimicrobial targets for NFGNRs. Dipeptidyl aminopeptidases (DPPs) are the primary enzyme for peptide digestion on the cell walls of NFGNRs. Here we report the high-resolution complex structure of PgDPP11 with citrate and potassium ions from a space-grown crystal (PDB ID: 6JTB); this structure is useful for generating a 3D pharmacophore model.

We previously reported that *in silico* docking of a Leu-Asp (LD) dipeptide into the active site of PgDPP11 suggested particular interactions between the bound dipeptide and the S1 subsite of PgDPP11 [1]. The putative oxyanion hole that stabilizes the negative charge on the scissile peptide carbonyl oxygen is formed with Ser655 and Gly653 as is formed by the backbone amide nitrogen atoms of Ser195 and Gly193 in chymotrypsin. In this study, we report the high-resolution crystal structure of PgDPP11 complexed with citrate and potassium ions from a space-grown crystal obtained in the Japanese experimental module “Kibo” at the International Space Station [2]. The most notable observation in this study is that one citrate ion was accommodated in the S1 subsite [Fig. 1(A)]. A distal carboxy group of the citrate ion forms a bifurcated salt bridge with the side chain of Arg673 and mimics the binding mode of the acidic (Asp / Glu) side chain of the P1 residue of the substrate peptide. Also, a water molecule which is hydrogen bonded to the central carboxy group of the citrate is adapted in the oxyanion hole of PgDPP11 and a potassium ion is stabilized by a cation- $\pi$  interaction with the indole ring of Trp219. These characteristics would be a good pharmacophore model for designing selective inhibitors with negatively charged groups. We

created a three-dimensional pharmacophore model on the basis of the distal carboxy of citrate, a water molecule bound to the central carboxy group of the citrate, and a potassium ( $K^+$ ) ion in a space-grown crystal-derived high-resolution crystal structure of the PgDPP11/citrate complex using the Unity module implemented in SYBYL-X Suite (Certara USA Inc., Princeton, NJ, USA). Two hydrogen bond acceptor (HBA) features were defined: at the centroid of two oxygen atoms based on the distal carboxy group of citrate and at the position of the oxygen atom of the water placed at the oxyanion hole. Likewise, one hydrogen bond donor (HBD) feature was defined based on the position of the  $K^+$  ion, since this position was suggested to correspond to the positively charged N-terminus of the P2 position of the substrate peptide. This pharmacophore was further employed for 3D pharmacophore-based virtual screening of compounds from the chemical database (namiki201306HTS) of Namiki Shoji Co., Ltd. (Tokyo, Japan), which contains 4 million compounds. The compounds were subsequently filtered by molecular weights of less than 300. As a result, 14,676 compounds were obtained as “first hits” from the model. Next, molecular docking was performed using Schrödinger Suite 2013-2 (Schrödinger, LLC, New York, NY, USA). The crystal



**Figure 1:** (A) Binding mode of citrate ion (orange) and potassium ion (purple) with Coulombic surface coloring from  $-10$  kcal/(mol $\cdot$ e) (red) to  $10$  kcal/(mol $\cdot$ e) (blue) using a dielectric constant of 4.0 in the PgDPP11 S1 subsite. (B) Binding mode of SH-5 (sky blue) in the PgDPP11 S1 subsite from docking study. (C) Binding mode of SH-5 (purple) in the PgDPP11 S1 subsite from crystal structure.

**Table 1:** Inhibitory effects of SH-5 and NPPB against S46 DPPs.

Enzyme	SH-5		NPPB	
	Residual Activity (%)	K <sub>i</sub> ( $\mu$ M)	Residual Activity (%)	K <sub>i</sub> ( $\mu$ M)
PgDPP11	62.9 $\pm$ 0.1	8.5 $\pm$ 0.4	70.3 $\pm$ 0.7	15.0 $\pm$ 0.7
SmDPP11	48.0 $\pm$ 1.1	24.9 $\pm$ 0.5	67.7 $\pm$ 0.6	84.8 $\pm$ 3.1
PgDPP7	54.4 $\pm$ 0.7	52.2 $\pm$ 3.3	159 $\pm$ 5	ND
SmDPP7	72.8 $\pm$ 0.7	36.6 $\pm$ 1.3	119.0 $\pm$ 0.3	ND

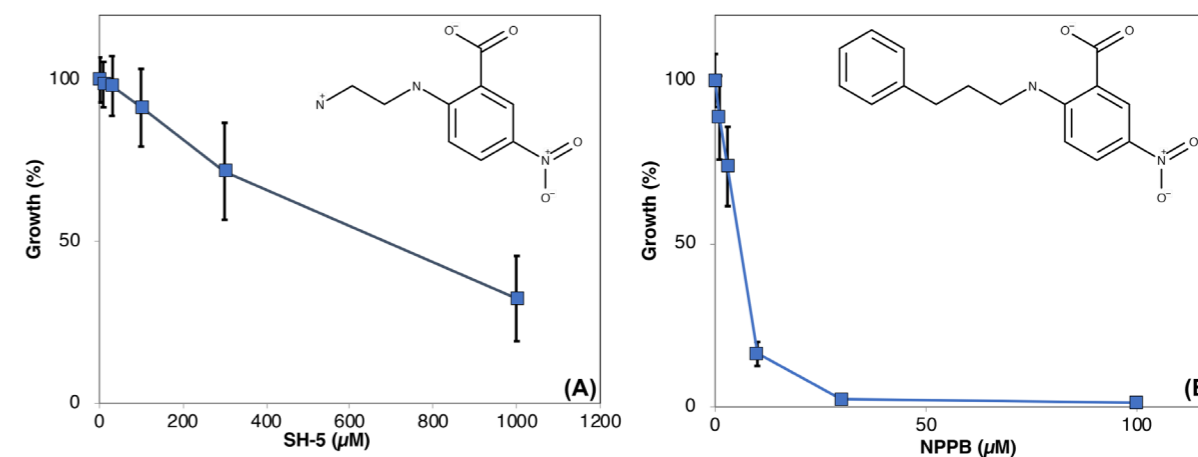


**Figure 2:** (A) Growth inhibition of Pg by SH-5. (B) Growth inhibition of Pg by NPPB. (The chemical structure of each compound is shown in the box.)

structure of PgDPP11 described above was used as a receptor for docking. As a result, the inhibitory effects of the 13 commercial candidate compounds obtained by the *in silico* screening were evaluated against the enzymatic activity of PgDPP11 on the synthetic substrate Leu-Asp-MCA. Among the 13 candidate compounds, only SH-5 (2-[(2-aminoethyl)amino]-5-nitrobenzoic acid, C<sub>9</sub>H<sub>11</sub>N<sub>3</sub>O<sub>4</sub>, Mw: 256.2) showed a significant inhibitory effect (>30% ca) against S46 DPPs (Table 1). Subsequently, we determined the crystal structure of PgDPP11 complexed with SH-5 using a space-grown crystal. The crystal structure revealed that the *in silico* docking model based on MM-GBSA scoring properly expressed the crystal structure [Fig. 1(B), (C)]. The inhibitory effect of SH-5 and a lipophilic structural analog of SH-5: NPPB (5-nitro-2-(3-phenylpropylamino)benzoic acid, C<sub>16</sub>H<sub>16</sub>N<sub>2</sub>O<sub>4</sub>, Mw: 300.31) against PgDPP11 was evaluated. The K<sub>i</sub> values of SH-5 and NPPB were estimated to be approximately 8.45 and 15.0  $\mu$ M, respectively. SH-5 and NPPB showed a dose-dependent inhibitory effect against the growth of *P. gingivalis* W83, but not on *E. coli* K12 (118.8%  $\pm$  5.6 at SH-5 1 mM, 98.1%  $\pm$  9.3 at NPPB 100  $\mu$ M) [Fig. 2(A), (B)]. However, a relatively high concentration of the inhibitor was required for SH-5. Interestingly, NPPB showed a relatively strong inhibitory effect against Pg. We have discovered SH-5 as the first non-peptidyl inhibitor of S46 peptidases by fragment-based *in silico* screening [3]. The high-resolution crystal structure from the space-grown crystals was

very useful for setting up a pharmacophore model and docking simulations for the *in silico* screening. Currently, we are proceeding with cytotoxicity evaluation of some candidate compounds for non-clinical studies. This research may open up a new horizon for structure-based inhibitor design including drug discoveries for proteases such as TMPRSS2 and DPP4 which are the target molecules of SARS-CoV2 and MERS-CoV, respectively, which have been attracting attention in recent months.

### REFERENCES

- [1] Y. Sakamoto, Y. Suzuki, I. Iizuka, C. Tateoka, S. Roppongi, M. Fujimoto, K. Inaka, H. Tanaka, M. Yamada, K. Ohta, H. Gouda, T. Nonaka, W. Ogasawara and N. Tanaka, *Sci Rep.* **5**, 11151 (2015).
- [2] I. Yoshizaki, M. Yamada, M. Iwata, M. Kato, K. Kihira, T. Ishida, Y. Wada and S. Nagao *Int. J. Microgravity Sci. and Appl.* **36**, 360101 (2019).
- [3] Y. Sakamoto, Y. Suzuki, A. Nakamura, Y. Watanabe, M. Sekiya, S. Roppongi, C. Kushibiki, I. Iizuka, O. Tani, H. Sakashita, K. Inaka, H. Tanaka, M. Yamada, K. Ohta, N. Honma, Y. Shida, W. Ogasawara, M. Nakanishi-Matsui, T. Nonaka, H. Gouda and N. Tanaka *Sci Rep.* **9**, 13587 (2019).

### BEAMLINE

BL-17A

Y. Sakamoto<sup>1</sup>, Y. Suzuki<sup>2</sup>, A. Nakamura<sup>3</sup>, M. Sekiya<sup>1</sup>, W. Ogasawara<sup>3</sup> and N. Tanaka<sup>4</sup> (Iwate Medical Univ., <sup>2</sup>Nagaoka Inst. of Tech., <sup>3</sup>Nagaoka Univ. of Tech., <sup>4</sup>Kitasato Univ.)